Efficient long-range collisional energy transfer between the E0g+(3P2) and D0u+(3P2) ion-pair states of I2, induced by H2O, observed using high-resolution Fourier transforn emission spectroscopy

AIP | The Journal of Chemical Physics

Efficient long-range collisional energy transfer between the E0g+(3P2) and D0u+(3P2) ion-pair states of I2, induced by H2O, observed using high-resolution Fourier transform emission spectroscopy

Trevor Ridley, Kenneth P. Lawley, Robert J. Donovan, and Amanda J. Ross

Citation: J. Chem. Phys. **135**, 114302 (2011); doi: 10.1063/1.3638267
View online: http://dx.doi.org/10.1063/1.3638267
View Table of Contents: http://jcp.aip.org/resource/1/JCPSA6/v135/i11
Published by the American Institute of Physics.

Efficient long-range collisional energy transfer between the $E0_g^+(^3P_2)$ and $D0_u^+(^3P_2)$ ion-pair states of I_2, induced by H_2O, observed using high-resolution Fourier transform emission spectroscopy

Trevor Ridley,[1,a)] Kenneth P. Lawley,[1] Robert J. Donovan,[1] and Amanda J. Ross[2]
[1]*EaStCHEM School of Chemistry, Joseph Black Building, The King's Buildings, Edinburgh EH9 3JJ, United Kingdom*
[2]*Université de Lyon, F-69622, Lyon, Université Lyon 1 & CNRS, UMR 5579 LASIM, 43 Bd du 11 Novembre 1918, Villeurbanne, France*

(Received 24 May 2011; accepted 28 July 2011; published online 16 September 2011)

Using high-resolution Fourier transform emission techniques, we have resolved rotational structure in the $D0_u^+(^3P_2) \rightarrow X0_g^+$ emission following collisional transfer from the $E0_g^+(^3P_2)$ state in I_2. The *P*:*R* branch ratios in the $E0_g^+(^3P_2) \rightarrow D0_u^+(^3P_2)$ transfer are found to vary enormously with v_E and v_D. We show that the observed intensities are all consistent with the transfer being dominated by long-range, near-resonant collisions with residual H_2O. Unequal *P*:*R* branch ratios in the $E0_g^+(^3P_2) \rightarrow A1_u$ emission have been shown to result from mixing of the $E0_g^+(^3P_2)$ and $\beta 1_g(^3P_2)$ states via Ω-uncoupling. © *2011 American Institute of Physics*. [doi:10.1063/1.3638267]

I. INTRODUCTION

In a recent paper,[1] we reported long-range (resonant) energy transfer between *g*/*u* ion-pair states of molecular iodine, e.g., $E0_g^+(^3P_2) \rightarrow D0_u^+(^3P_2)$, induced by collisions with H_2O via dipole coupling. The large rate constants deduced for collisional transfer between a range of vibrational levels of the two states, up to 5×10^{-9} molecules^{-1} cm^3 s^{-1}, can be two orders of magnitude greater than that for transfer between the same two levels following collisions with $I_2(X)$. Consequently, it was proposed that H_2O desorbed from the walls of the sample cell or from solid I_2 itself could have significantly affected the results of earlier studies of collisional transfer by supposedly dry $I_2(X)$ previously reported in the literature. The large rate constants required at such low partial pressures of H_2O were shown to be possible with long-range, near-resonant interactions that arise when there is close matching of the energy change in the ion-pair states, $\Delta E(I_2)$, with the change in energy that accompanies a rotational transition in the ground state of H_2O, $\Delta E(H_2O)$. This dipole-induced electronic transition must be accompanied by $\Delta J = \pm 1$ and a dipole-allowed transition in H_2O to fulfil the conditions for rapid energy transfer.

The requirement[1] that these energy mismatches, ΔE^*, $(\Delta E(I_2) - \Delta E(H_2O))$, be ≤ 5 cm^{-1} (and ≤ 2 cm^{-1} for a detailed rate constant $\geq 10 \times 10^{-9}$ molecules^{-1} cm^3 s^{-1}) suggests that the intensity of emission from pairs of levels populated by $\Delta J = \pm 1$, for $E0_g^+(^3P_2) \rightarrow D0_u^+(^3P_2)$ collisional transfer should, according to the model, be very unequal. This will become more likely as the branch separation increases at higher *J* values, and also as the resonant transitions required from H_2O move to higher energies where the density of possible transitions (far-IR lines) is less. This energy matching criterion is based on collisions occurring with the most probable relative velocity, v^*, at room temperature. Doubling the collision velocity to, say, $2v^*$ would double the value of ΔE^* to preserve the same value of the Massey parameter, $\Delta Eb/\hbar v$, at a given impact parameter, *b*. However, ΔE^* would then be an even smaller fraction of the relative kinetic energy. These collisions in the tail of the Maxwell-Boltzmann distribution would have the effect of slightly reducing inequalities in the *P*:*R* branch ratios.

In our earlier work,[1] each vibronic band in the $D0_u^+(^3P_2) \rightarrow X0_g^+$ emission was composed of four lines, a *P* and *R* branch from each of the two collisionally populated rotational levels. However, it was not possible to resolve these lines and, hence, determine whether the populations of the two collisionally populated levels were different.

However, such data are available in a much earlier study,[2] in which Fourier transform (FT) detection was used. Rotational structure was resolved in $D0_u^+(^3P_2) \rightarrow X0_g^+$ emission that was also observed following collisional transfer from the $E0_g^+(^3P_2)$ state which had been selectively excited by optical-optical double resonance (OODR). These spectra were recorded with the specific aim of obtaining molecular constants for the $C1_u$ valence state (called $B''1_u$ in Ref. 2 and some earlier studies but relabelled to be consistent with the notation used for the other halogens). As it was not possible to record any new spectra with this experimental arrangement, we were restricted to re-examining the original data in the light of our recent study.[1] Consequently, the ideal (*v*, *J*) combinations are not always available.

In the FT experiments,[2] considerable effort was made to remove traces of H_2O and other impurities (see below), and hence, it was assumed that all H_2O would have been removed from the sample cell. Spectra recorded under these conditions will subsequently be described as "dry." However, many FT spectra were also recorded before these measures were taken to remove H_2O and these will be described as "wet." In

a)Author to whom correspondence should be addressed. Electronic mail: T.Ridley@ed.ac.uk. Fax: +44-131-6506453.

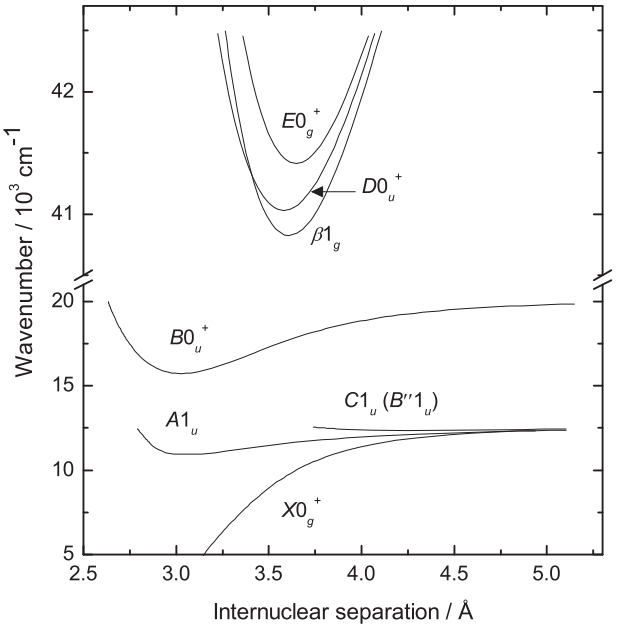

FIG. 1. Potential energy curves of the electronic states of I_2 discussed in this work. The curves were generated from the results of Martin *et al.* (Ref. 5) ($X0_g^+$), Viswanathan *et al.* (Ref. 6) ($A1_u$), Inard *et al.* (Ref. 2) ($C1_u$), Luc (Ref. 7) ($B0_u^+$), Perrot *et al.* (Ref. 8) ($\beta 1_g$), Tellinghuisen (Ref. 9) ($D0_u^+$), and Brand *et al.* (Ref. 10) ($E0_g^+$). The $C1_u$ state has a shallow minimum around 4.2 Å.

the present paper, we will present some of these unpublished spectra and show that the intensities of the rotational lines are very irregular and that these intensities are entirely consistent on a quantitative basis with them being determined by long-range, near-resonant interactions with ground state H_2O. In addition, we will propose that even in the previously published "dry" spectrum the $E0_g^+(^3P_2) \rightarrow D0_u^+(^3P_2)$ transfer is still dominated by collisions with H_2O. A different mechanism involving dipole-induced electronic transitions by collisions with free electrons has recently been proposed for the irregular intensities of the rotational lines,[3] but no quantitative estimate was given of the electron densities required, or any rotational branch selectivity that might result.

A second imbalance in rotational line intensities was observed in the previous FT study.[2] It could be clearly seen that while the *P:Q:R* branch ratios in the direct $E0_g^+(^3P_2) \rightarrow C1_u$ emission were as expected, those in the $E0_g^+(^3P_2) \rightarrow A1_u$ emission were not, but this observation was not commented on by the authors. In this case, we will propose that the imbalance is due to Ω-uncoupling between the $E0_g^+(^3P_2)$ and $\beta 1_g(^3P_2)$ states, first reported in absorption by Perrot *et al.*[4] Potential energy curves of all of the relevant states[2,5–10] are shown in Fig. 1.

II. EXPERIMENTAL

High- and low-resolution dispersed emission spectra were recorded in Lyon and Edinburgh, respectively. In both cases, various $E0_g^+(^3P_2)$ state levels of I_2 were excited from the $X0_g^+$ ground state by (1+1′) OODR via the $B0_u^+$ state.

In Lyon, the pump and probe photons were generated by CW single-mode ring dye lasers (Spectra-Physic 380-D). The pump laser operating with Rhodamine 110 dye was pumped by a Spectra-Physics 2045-15 Ar^+ laser, with a Spectra-Physics 381 interferometer (equipped with a scanning driver) providing a frequency mode monitor. The probe laser operating with Stilbene 3 was interferometrically stabilized with a Spectra-Physics 388 Stabilok system and pumped by an INNOVA 200-K3 Kr^{2+} laser. The wavelengths of the dye laser outputs were controlled using a Laser Technics 100 Fizeau wavemeter.

The pump and probe photons were superimposed using a dichroic mirror and then focussed with an $f = 25$ cm lens into the sample cell. Back-scattered I_2 fluorescence was collected on a pierced mirror and focussed with an $f = 10$ cm lens on to the entrance aperture of a BOMEM DA3 FT spectrometer equipped with a UV quartz beamsplitter and an EMI 9558 QB photomultiplier. The intensities are accurate to approximately ±10%.

In order to remove traces of H_2O and other impurities from the walls, the cell was heated to 500 °C under evacuating pressures below 10^{-6} Torr using a diffusion pump with a liquid N_2 cold trap. Reagent grade I_2 was introduced by distillation onto the liquid N_2-cooled cell walls and subjected to several freeze-pump-thaw cycles.

In Edinburgh, a XeCl excimer laser (Lambda Physik EMG 201MSC) simultaneously pumping two Lambda Physik dye lasers generated the pump and probe photons. The unfocussed, counter-propagating, temporally overlapped pump and probe beams were directed through the sample cell. The emission, at 90° to the laser beams, was dispersed by a Jobin-Yvon HRS2 (f/7, 0.6 m) monochromator and monitored by a Hammamatsu R928 photomultiplier tube. The output from the photomultiplier was processed by a Stanford Research SR250 gated integrator and stored on a PC.

The glass cell fitted with Spectrosil quartz entrance/exit windows using halocarbon wax was evacuated with a rotary-backed turbo pump to a base pressure of $<1 \times 10^{-3}$ Torr. The solid I_2 was held in a side arm of the cell that could be closed to the cell by a tap. Spectra recorded within one hour of refilling the cell, where the effects of collisions with H_2O were minimized,[1] will be described as "dry." This was taken to be the conditions under which the minimum integrated collision-induced emission was observed. Although strenuous attempts were made to remove water/impurities in the Lyon experiments, it is not clear if desorption of H_2O as a function of time affected these studies in the same way as it did for those carried out in Edinburgh. The spectra in both Lyon and Edinburgh were all recorded with I_2 at its vapor pressure (~0.2 Torr at 293 K).

III. RESULTS AND DISCUSSION

A. Collisional transfer by H_2O

An example of a "dry" low-resolution emission spectrum, recorded by exciting $E(v = 8, J = 55)$, is shown in Fig. 2(a). With the exception of part of the broad band around 325 nm, all the emissions above 320 nm in the spectrum are due to $E0_g^+(^3P_2) \rightarrow A1_u$. Very weak $D0_u^+(^3P_2) \rightarrow X0_g^+$ emission resulting from $E0_g^+(^3P_2) \rightarrow D0_u^+(^3P_2)$

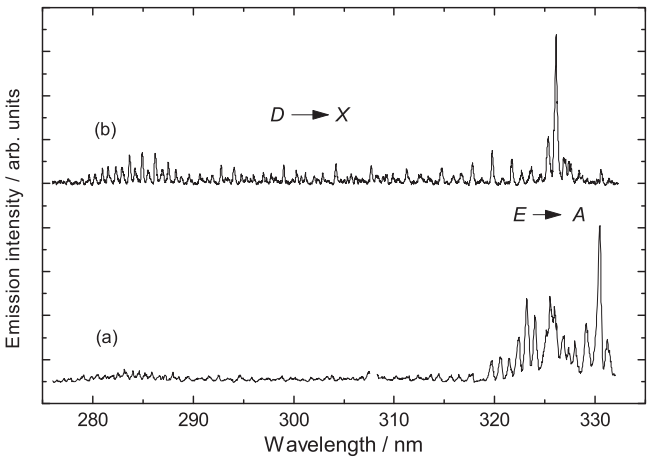

FIG. 2. Low-resolution emission between 270 and 333 nm following the excitation of $E(v = 8, J = 55)$ recorded (a) immediately after refilling the cell, "dry," and (b) with 0.03 Torr of H_2O added. The intensities of the spectra are normalized to the most intense peaks.

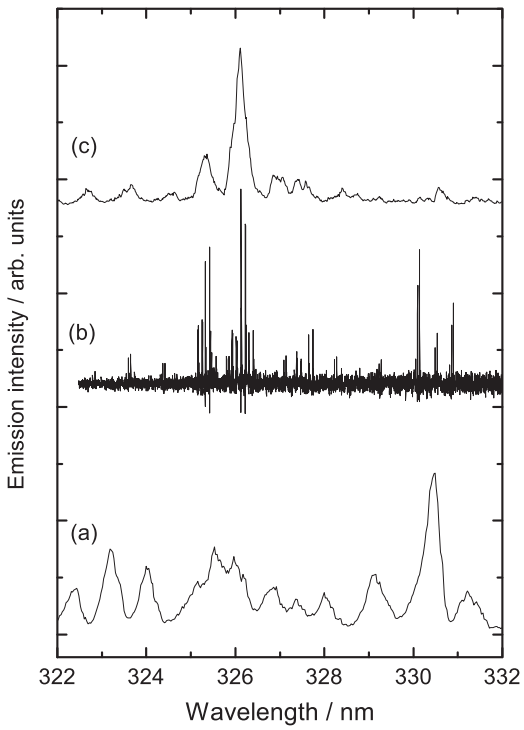

FIG. 3. Expansions of the low-resolution emission between 322 and 332 nm following the excitation of $E(v = 8, J = 55)$; (a) "dry" and (c) with 0.03 Torr of H_2O added. The "wet," high-resolution FT emission following excitation of $E(v = 8, J = 98)$ is shown in (b). The intensities of the spectra are normalized to the most intense peaks.

collisional transfer is observed down to 275 nm which is the low-wavelength limit of the emission from the vibrational levels populated ($v_D = 10-13$). Previously,[1] we showed that, under these conditions, the $E0_g^+(^3P_2) \rightarrow D0_u^+(^3P_2)$ transfer is dominated by collisions with $I_2(X)$. The spectrum in Fig. 2(b) was recorded with 0.03 Torr of H_2O added. Here, the integrated $D0_u^+(^3P_2) \rightarrow X0_g^+$ emission, extending between 275 and 330 nm, is now an order of magnitude more intense than the $E0_g^+(^3P_2) \rightarrow A1_u$ emission.

Expansions of the 322–332 nm region of the spectra shown in Figs. 2(a) and 2(b) are shown in Figs. 3(a) and 3(c), respectively. The same wavelength region of the "wet," high-resolution FT emission following excitation of $E(v = 8, J = 98)$ is shown in Fig. 3(b). The relative intensity distribution observed in the FT emission appears to be intermediate between those observed in the two low-resolution spectra. The two largest peaks in the spectra of "dry" I_2 and I_2 with H_2O added lie at 330.5 nm, $E0_g^+(^3P_2) \rightarrow A1_u$, and 326 nm, $D0_u^+(^3P_2) \rightarrow X0_g^+$, respectively; both peaks are very small in the complementary spectra. In the high-resolution FT spectrum, two sets of bands are observed centred at the same wavelengths but with nearly equal intensities, suggesting that there is residual H_2O present.

Furthermore, the relative contributions of the $D0_u^+(^3P_2)$ state vibrational levels, N_v, observed in the high-resolution spectrum are 0.3, 1, 0.5, and 0 for N_{10}, N_{11}, N_{12}, and N_{13}, in agreement with the distributions that we observed previously for transfer by H_2O. In contrast, the equivalent distributions observed for transfer by $I_2(X)$ were 0.5, 1, 0.9, and 0.6. Hence, it is concluded that the $E0_g^+(^3P_2) \rightarrow D0_u^+(^3P_2)$ transfer that gives rise to the emission shown in Fig. 3(b) is predominantly induced by collisions with ground state H_2O and not $I_2(X)$. This is not surprising as the measured rate constants for $E(v = 8, J = 55)$ are 0.2×10^{-10} and 33×10^{-10} molecules^{-1} cm^3 s^{-1} for collisional transfer by $I_2(X)$ and H_2O, respectively.[1]

A further amplification of two segments of the FT spectrum, together with the assignments of the $D0_u^+(^3P_2) \rightarrow X0_g^+$, rovibronic transitions, determined from published molecular constants,[5,9] is shown in Fig. 4. It can be seen that the intensity of the emission from pairs of levels populated by $\Delta J = \pm 1$, $E0_g^+(^3P_2) \rightarrow D0_u^+(^3P_2)$, collisional transfer varies enormously. For example, emission is seen almost exclusively from $J = 97$ of $D(v = 10)$; for $D(v = 11)$, emission from $J = 97$ is approximately three times more intense than from $J = 99$ and for $D(v = 12)$, the emissions from $J = 97$ and $J = 99$ have approximately the same intensity. The spectra in Figs. 4(a) and 4(b) from the same upper state exhibit the same intensity patterns to adjacent vibrational levels in the ground state.

To a first approximation, the same marked branch imbalance is true for all of the pairs of $D0_u^+(^3P_2)$ state rotational levels that we conclude are populated by long-range collisional transfer from all of the other $E0_g^+$ state vibrational levels that were excited, namely, $E(v = 7, 5, 3, 1,$ and $0)$. An example of the $D0_u^+(^3P_2) \rightarrow X0_g^+$ emission following excitation of $E(v = 7, J = 31)$ is shown in Fig. 5 and the intensity data are summarized in Table I.

The term values of the rotational levels relevant to the high-resolution spectrum are shown in Table I. The energy changes, $\Delta E(I_2)$, associated with collisional transfer between the ion-pair states are also shown and can be compared with the energy changes, $\Delta E(H_2O)$, associated with intense rotational transitions in H_2O at room temperature.[11] Randall *et al.*[11] tabulated the intensities of the lines, in a scale of 0.1–300, observed between 75 and 550 cm^{-1} in the absorption spectrum of H_2O. In the present paper, intense transitions are arbitrarily chosen to have intensities ≥ 50. The values for $\Delta E(H_2O)$ of ≤ 75 cm^{-1} are calculated from the

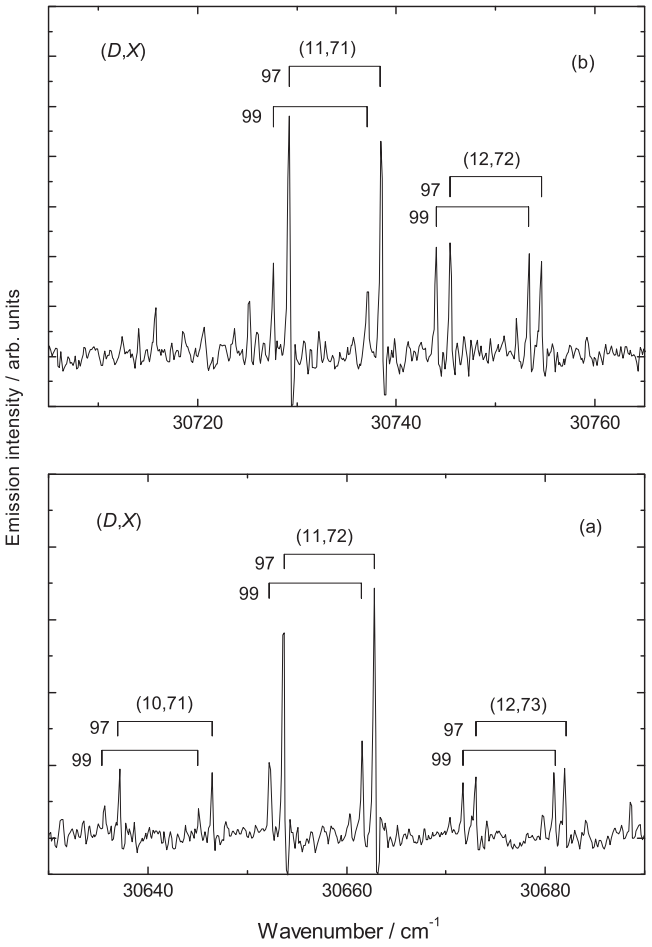

FIG. 4. Two segments of the FT $D0_u^+(^3P_2) \rightarrow X0_g^+$ emission following the excitation of $E(v = 8, J = 98)$. The labels identify vibrational quantum numbers in the (D,X) bands and rotational numbering in the $D0_u^+(^3P_2)$ state.

rotational energy levels[11] for $J'_{\tau'} - J''_{\tau''}$ transitions where $J'_{\tau'}$ has a rotational energy $\leq$500 cm^{-1} and only those for which $\Delta J = 0, \pm 1$, $\Delta\tau = 0, \pm 2$ as these characterize the strongest transitions.

The energy mismatches, $\Delta E(I_2) - \Delta E(H_2O)$, explain, at least semi-quantitatively, the observed emission intensities.

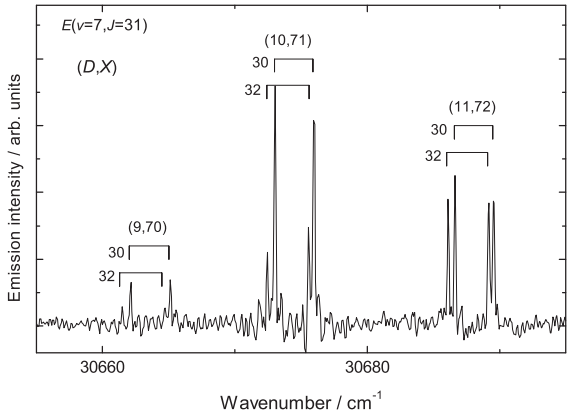

FIG. 5. Part of the FT $D0_u^+(^3P_2) \rightarrow X0_g^+$ emission following the excitation of $E(v = 7, J = 31)$. The labels identify vibrational quantum numbers in the (D,X) bands and rotational numbering in the $D0_u^+(^3P_2)$ state.

TABLE I. The term values, relative to $X(v = 0, J = 0)$, of rovibronic levels of the $D0_u^+(^3P_2)$ state (Ref. 9), the energy change, $\Delta E(I_2)$, associated with collisional transfer from various rovibronic levels of the $E0_g^+(^3P_2)$ state (Ref. 10), the relative intensity of the emission from the level populated, I, and the energy change, $\Delta E(H_2O)$, associated with the most intense rotational transitions in the ground state of H_2O (Ref. 11). Only H_2O transitions where the energy mismatch, $\Delta E(I_2) - \Delta E(H_2O)$, $\leq$5 cm^{-1} are included; those where it is $\leq$2 cm^{-1} are shown in bold type. The values for $\Delta E(H_2O)$ of $\geq$75 cm^{-1} are taken from the experimental data (Ref. 11), while those of $\leq$75 cm^{-1} are calculated from the rotational energy levels (Ref. 11) for $J'_{\tau'} - J''_{\tau''}$ transitions where $J'_{\tau'}$ has a rotational energy $\leq$500 cm^{-1} and only those for which $\Delta J = 0, \pm 1$ and $\Delta\tau = 0, \pm 2$, as these characterize the strongest transitions.

(i) $E(v = 8, J = 98; 42\,341.0$ cm$^{-1})$; see Fig. 4

v	$J = 97/99$/cm^{-1}	$\Delta E(I_2)$/cm^{-1}	I	$\Delta E(H_2O)$/cm^{-1}
10	42 096.9	244.1	1	248.0
				245.6
	42 104.9	236.1	0.1	...
11	42 188.9	152.1	1	**153.6**
				151.4
				150.6
				149.2
	42 196.9	144.1	0.3	140.8
				139.8
				139.1
12	42 280.7	60.3	1	64.1
				64.0
				58.0
				57.4
				55.6
				55.4
	42 288.7	52.3	1	55.6
				55.4
				53.3
				51.4
				51.3

(ii) $E(v = 7, J = 31; 42\,073.2$ cm$^{-1})$; see Fig. 5

v	$J = 30/32$/cm^{-1}	$\Delta E(I_2)$/cm^{-1}	I	$\Delta E(H_2O)$/cm^{-1}
9	41 831.0	242.2	1	245.6
	41 833.5	239.7	...	...
10	41 923.7	149.5	1	153.6
				151.4
				150.6
				149.2
	41 926.3	146.9	0.3	151.4
				150.6
				149.2
11	42 016.1	57.1	1	**58.0**
				57.4
				55.6
				55.4
				53.3
	42 018.6	54.6	1	58.0
				57.4
				55.6
				55.4

TABLE I. *(Continued.)*

				53.3
				51.4
				51.3
(iii) $E(v = 5, J = 36; 41\,882.4\ cm^{-1})$				
v	$J = 35/37/cm^{-1}$	$\Delta E(I_2)/cm^{-1}$	I	$\Delta E(H_2O)/cm^{-1}$
7	41 651.6	230.8	0.3	227.9
				226.4
	41 654.5	227.9	1	**227.9**
				226.4
				223.8
8	41 744.8	137.6	1	140.8
				139.8
				139.1
				132.7
	41 747.8	134.6	1	139.1
				132.7
9	41 837.7	44.7	1	47.1
				47.1
				41.1
				40.5
	41 840.6	41.8	1	**41.1**
				40.5
				38.7
				38.5
				37.1
(iv) $E(v = 3, J = 72; 41\,761.0\ cm^{-1})$				
v	$J = 71/73/cm^{-1}$	$\Delta E(I_2)/cm^{-1}$	I	$\Delta E(H_2O)/cm^{-1}$
4	41 449.6	311.4	0.4	...
	41 455.5	305.5	1	303.3
				303.0
5	41 543.4	217.6	1	221.8
	41 549.3	211.7	1	208.5
6	41 636.8	124.2	1	127.0
				122.0
				120.2
	41 632.8	118.2	0.8	122.0
				120.2
(v) $E(v = 1, J = 35; 41\,481.4\ cm^{-1})$; see Fig. 7(a)				
v	$J = 34/36/cm^{-1}$	$\Delta E(I_2)/cm^{-1}$	I	$\Delta E(H_2O)/cm^{-1}$
2	41 180.7	300.7	1	303.2
				303.0
	41 183.6	297.8	0.5	...
3	41 275.0	206.4	0.5	208.5
				203.1
				202.8
				202.6
	41 278.0	203.4	1	**203.1**
				202.8
				202.6
4	41 369.2	112.2	1	**111.2**
	41 372.1	109.3	1	**111.2**
				104.6

TABLE I. *(Continued.)*

(vi) $E(v = 0, J = 63; 41\,435.7\ cm^{-1})$				
v	$J = 62/64/cm^{-1}$	$\Delta E(I_2)/cm^{-1}$	I	$\Delta E(H_2O)/cm^{-1}$
1	41 142.1	293.6	0.8	289.7
	41 147.4	288.3	1	**289.7**
2	41 236.6	199.1	1	203.1
				202.8
				202.6
				194.5
	41 241.8	193.9	0.7	**194.5**
3	41 330.8	104.9	0.8	**104.6**
				100.6
	41 336.0	99.7	1	104.6
				100.6
				99.0

For example; following excitation of $E(v = 8, J = 98)$, for $D(v = 10)$, the collisional transfer to $J = 97$ is enhanced by one rotational transition in H_2O with an energy mismatch of $<2\ cm^{-1}$ and another of $<5\ cm^{-1}$, but there is no such transition in H_2O that can enhance the transfer to $J = 99$. Hence, almost no emission is observed from $J = 99$ in the (10,71) vibronic band in Fig. 4(a). From a similar consideration of the energy mismatches involved, it can be predicted that for $D(v = 11)$, the transfer to $J = 97$ should be enhanced more than to $J = 99$ and for $D(v = 12)$ the two transitions should be equally enhanced. The intensities observed in the (11,71), (11,72) (12,72), and (12,73) vibronic bands are consistent with these predictions. It would be a remarkable coincidence, if the relative intensities of the ten pairs of *P*/*R* lines studied could be predicted as accurately as illustrated in Table I in case they were being determined by anything other than resonant collisions with H_2O. The same criteria can be used to explain the intensities observed in all of the spectra obtained by exciting various $E(v, J)$ levels, including $E(v = 7, J = 31)$, shown in Fig. 5.

On the basis of energy mismatches alone, it is predicted that there should also be effective transfer to $D(v = 13)$ from $E(v = 8)$. However, it was shown[1] that the probability of a particular transition is also dependent on the Franck-Condon (FC) overlap between the initial and final states. The FC overlaps between $E(v = 8)$ and $D(v = 10, 11, 12,$ and $13)$ are 0.344, 0.210, 0.021, and <0.001, respectively, and consequently, the transition probability to $D(v = 13)$ is very small.

There is another apparent anomaly in the values for the $E(v = 1) \rightarrow D(v = 2)$ collisional transfer, shown in Table I(v). Although some $\Delta J = +1$ collisional transfer is observed, no H_2O transitions lie inside the $5\ cm^{-1}$ window for $\Delta E(I_2) - \Delta E(H_2O)$ for the transition. However, there are two H_2O transitions with mismatches of 5.2 and 5.4 cm^{-1}, just outside the window, and this illustrates that the window is only used as a guide to the rate of the transfer and is not a threshold.

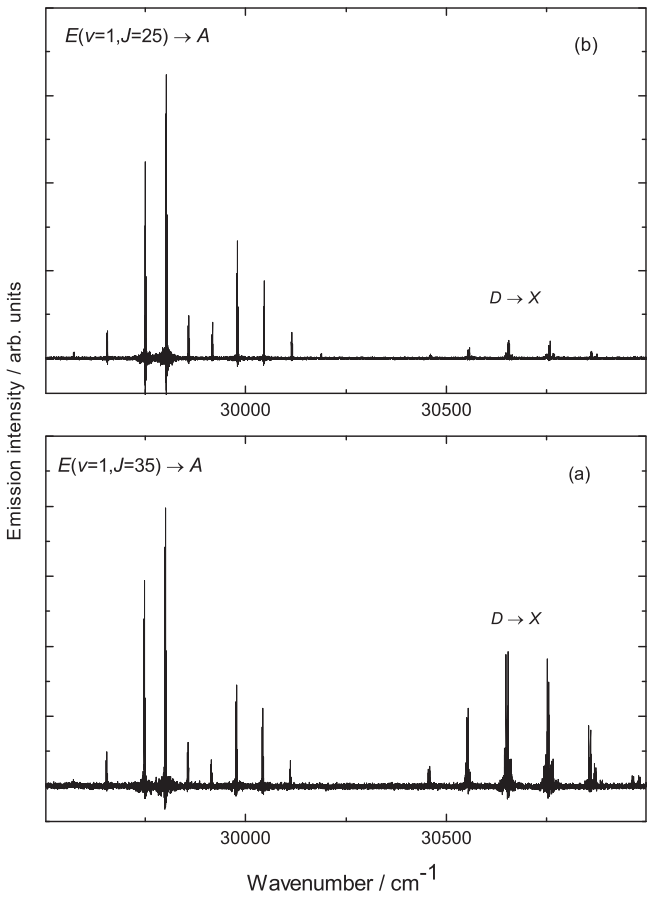

FIG. 6. The FT $E0_g^+(^3P_2) \rightarrow A1_u$ and part of the $D0_u^+(^3P_2) \rightarrow X0_g^+$ emission recorded (a) before and (b) after the drying process. The spectra in (a) and (b) were recorded by exciting $E(v = 1, J = 35)$ and $E(v = 1, J = 25)$, respectively.

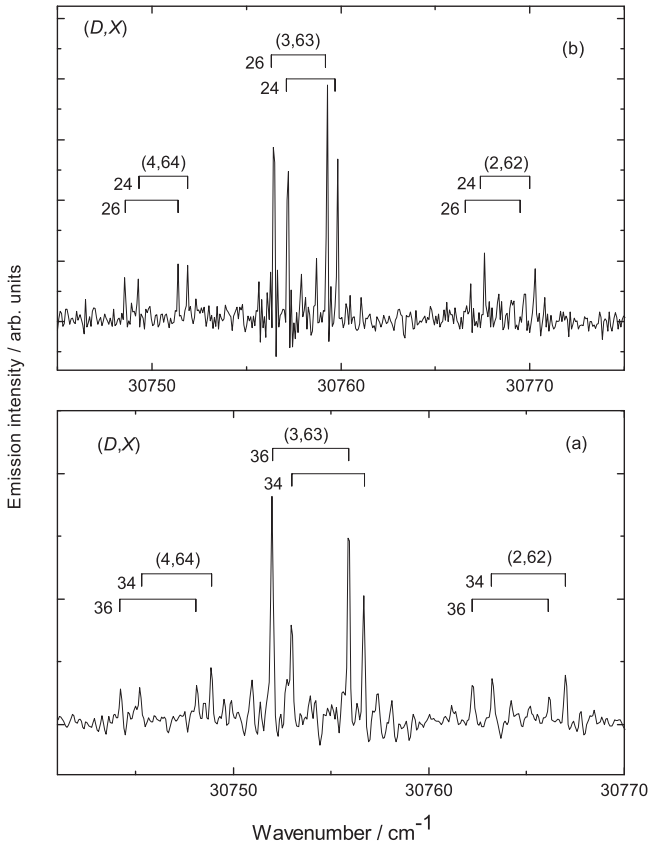

FIG. 7. Expansions of segments of the spectra shown in Figs. 6(a) and 6(b). The labels identify vibrational quantum numbers in the (D,X) bands, and rotational numbering in the $D0_u^+(^3P_2)$ state.

It should be emphasized that none of the six $E0_g^+(^3P_2)$ state vibrational levels excited are in near-resonance with a $D0_u^+(^3P_2)$ state level, and hence, the transfer by $I_2(X)$ will only involve short-range, non-resonant collisions. Under these conditions, the rate constant for transfer by $I_2(X)$ will be two orders of magnitude less than for transfer by H_2O.

A further illustration of how difficult it is to eliminate H_2O from these I_2 experiments is provided by a comparison of spectra recorded before and after the rigorous drying measures described above for the FT experiments were applied. An example of spectra recorded following excitation of $E(v = 1)$ is shown in Figs. 6 and 7. The spectra, normalized to the $E0_g^+(^3P_2) \rightarrow A1_u$ emission, recorded before and after the drying are shown in Figs. 6(a) and 6(b), respectively. Clearly, the relative intensity of the collision-induced $D0_u^+(^3P_2) \rightarrow X0_g^+$ emission has greatly been reduced by the drying.

An enlargement of one segment of these spectra is shown in Figs. 7(a) and 7(b), the latter being a reproduction of part of Fig. 3c of Ref. 2. Although it might be argued that there is a slight equalization of the intensities of the rotational lines in the "dry" spectrum, they are clearly still irregular, and hence, it has to be concluded that, in this example, collisions with H_2O are still having a significant effect on the $E0_g^+(^3P_2) \rightarrow D0_u^+(^3P_2)$ transfer, even after initial attempts at drying. At the time when the experiments were carried out in Lyon, the magnitude of the influence that H_2O can have on the spectra was not known and the effectiveness of the removal of "impurities" was judged solely on the minimization of the collision-induced $D0_u^+(^3P_2) \rightarrow X0_g^+$ emission. In the Edinburgh experiments, we had a second diagnostic for a truly "dry" spectrum (Figs. 2(a) and 3(a)), namely, the relative contributions of the emitting $D0_u^+(^3P_2)$ state vibrational levels as outlined above. It is possible that these conditions were never achieved in Lyon. Were the spectrum in Fig. 7(b), if not that in 7(a), to be caused predominantly by collisions with $I_2(X)$ this would mean that such collisions result in the same irregular intensities of rotational lines that are characteristic of collisions with H_2O which would be a remarkable coincidence.

However, as the pressure of H_2O decreases, a point will be reached when short range non-resonant collisional transfer by $I_2(X)$ will become competitive with long-range resonant transfer by H_2O. If non-resonant collisions with $I_2(X)$ have collision rates for $\Delta J = +1$ transitions that are the same as those for $\Delta J = -1$ transitions, as the conditions become "drier," the imbalance in the intensities of the emission from the collisionally populated pairs of lines will begin to diminish. This effect may explain any equalization of the intensities observed in Fig. 7(b) and also the rare minor inconsistencies in the intensities shown in Table I, e.g., the intensity of the $E(v = 3, J = 72) \rightarrow D(v = 4, J = 71)$ transfer seems to be larger than expected.

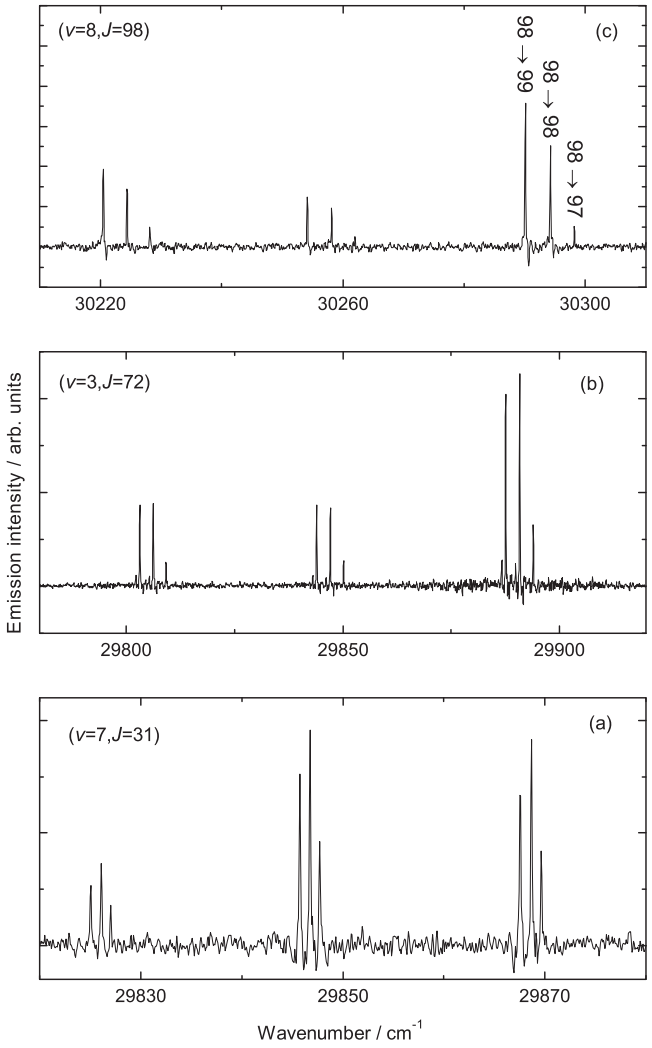

FIG. 8. Part of the FT $E0_g^+(^3P_2) \rightarrow A1_u$ emission following excitation of (a), $E(v = 7, J = 31)$, (b), $E(v = 3, J = 72)$, and (c), $E(v = 8, J = 98)$.

B. *R:Q:P* branch ratios in $E0_g^+(^3P_2) \rightarrow A1_u$ emission

An expansion of part of the $E0_g^+(^3P_2) \rightarrow A1_u$ emission following excitation of $E(v = 7, J = 31)$ is shown in Fig. 8(a). It can be seen that the *R:Q:P* branch ratios are not 1:2:1 as expected, with the *P* branch ($J = 31 \rightarrow 32$ emission line) being significantly more intense than the *R* branch. This phenomenon can be observed in the spectra shown by Inard *et al.*[2] but was not commented on by the authors. In all of the spectra that we recorded, the trend increases with *J*; two examples are shown in Figs. 8(b) and 8(c) to the extent that the *P* branch is the most intense in the emission from $J = 98$. Unfortunately, we do not have a complete series of spectra that shows how the *R:Q:P* branch ratios vary with *v* and *J*. In contrast, the *R:Q:P* branch ratios in the $E0_g^+(^3P_2) \rightarrow C1_u$ emission have the expected 1:2:1 values as can be seen from the spectra in Fig. 9.

Similar anomalous line intensities were reported by Perrot *et al.*[4] in fluorescence excitation spectra recorded by populating the $\beta 1_g(^3P_2)$ state via a $\Delta\Omega = 1$ transition from the $B0_u^+$ state. The spectra also showed inequalities in the

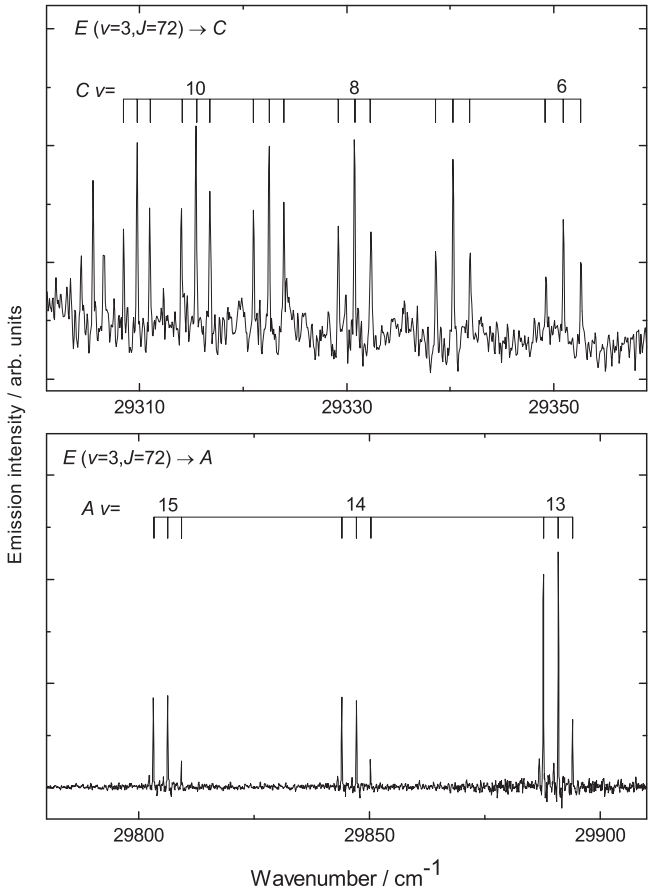

FIG. 9. Part of the FT $E0_g^+(^3P_2) \rightarrow A1_u$, and $E0_g^+(^3P_2) \rightarrow C1_u$, emissions following excitation of $E(v = 3, J = 72)$.

R:P branch ratios that increased with *J* but were almost invariant with *v*.

The observations were explained by vibrationally induced coupling between members of the close-lying $E0_g^+(^3P_2)$ and $\beta 1_g(^3P_2)$ vibrational manifolds. Interference between the parallel and perpendicular transitions depends on the relative phases of the two transition amplitudes. These change between the *P* and *R* branches, resulting in a departure of the *R:P* branch ratio from unity.[12]

In the experiments of Perrot *et al.*[4] the $\beta 1_g(^3P_2)$ state is directly accessed and each v_β level contains a small $E0_g^+(^3P_2)$ state component. In the present work, vibrational levels of the $E0_g^+(^3P_2)$ state are directly accessed and these contain a small $\beta 1_g(^3P_2)$ component. In both cases, the Ω-uncoupling operator,

$$V = -\frac{\hbar^2}{\mu R^2}\mathbf{J} \cdot (\mathbf{L} + \mathbf{S}), \tag{1}$$

is responsible for E/β mixing and the treatment of Perrot *et al.* is unchanged. A key requirement is that the transition dipole between the minor electronic component in the upper (lower) state to the major component in the lower (upper) state is much stronger than the transition dipole between the two major components. In the experiments of Perrot *et al.*, the strong transition was $E0_g^+(^3P_2) \leftarrow B0_u^+$ and the weak transition was $\beta 1_g(^3P_2) \leftarrow B0_u^+$; in the present experiments, the strong transition is $\beta 1_g(^3P_2) \rightarrow A1_u$ and the

weak transition is $E0_g^+(^3P_2) \rightarrow A1_u$.The extent of mixing is very small and the term values are not measurably perturbed. In principle, a given vibrational level of the $E0_g^+(^3P_2)$ state, v_E, is mixed with the complete manifold of v_β levels,

$$|\Omega, v_E\rangle = |0, v_E\rangle + \sum_{v_\beta} \alpha(v_E, v_\beta)|1, v_\beta\rangle, \quad (2)$$

with mixing coefficients $\alpha(v_E,v_\beta)$ given in 1st order by

$$\alpha(v_E, v_\beta) \approx -J B_v \frac{\langle 0_g^+|L_- + S_-|1_g\rangle}{E(v, J_E) - E(v, J_\beta)} \langle v_E|v_\beta\rangle, \quad (3)$$

where any J-dependence of the FC factor $\langle v_E, v_\beta\rangle$ has been ignored and the vibronic levels are assumed to have the same B value. Then, if the pure precession model is used for the ion-pair states, which must be in the same tier, Perrot *et al.*[4] find

$$\langle 0_g^+|L_- + S_-|1_g\rangle = 12. \quad (4)$$

The sign of $\alpha(v_E, v_\beta)$ depends on the sign of the denominator in Eq. (3). If the parent v_E level lies exactly mid-way between adjacent v_β levels, $\alpha(v_E, v_\beta - 1)$ and $\alpha(v_E, v_\beta)$ would have opposite signs (disregarding any difference in FC factors and ignoring sums over more distant vibrational levels). Their contribution to emission from the mixed state to a common lower electronic state would then cancel. In the present case, there is an imbalance in contributions from higher and lower energies to the sum over v_β in Eq. (2) and the effect is seen. For instance, for $v_E = 8$, the two adjacent v_β levels lie, respectively, 61 cm^{-1} below and 38 cm^{-1} above. Substituting these energy differences into Eq. (3) with $B = 0.02$ cm^{-1}, $J = 110$, and $\langle v_E, v_\beta\rangle = 0.1$ gives $\alpha(8,v_\beta-1) = 3.9 \times 10^{-2}$ and $\alpha(8,v_\beta) = 6.3 \times 10^{-2}$. Since the relative intensities of the $E0_g^+(^3P_2) \rightarrow A1_u$ and $\beta 1_g(^3P_2) \rightarrow A1_u$ systems is $\approx 10^{-2}$:1,[13] the two transition amplitudes from the mixed upper state have comparable strength and appreciable interference results.

The value $E(v_E) - E(v_\beta)$ only varies slightly over the (v, J) range studied. The two adjacent v_β rotationless levels lie 70–61 cm^{-1} below and 32–38 cm^{-1} above the rotationless levels of $v_E = 0$–8, respectively. In addition, the difference between the rotational energy for $J = 100$ in the coupled levels only varies by ~ 2 cm^{-1} over the same range of vibrational levels.

For the $E0_g^+(^3P_2) \rightarrow C1_u$ system shown in Fig. 9(b), the *R:Q:P* branch ratios are 1:2:1 as expected. Here, the transition dipole between the minor electronic component in the upper state to the major component in the lower state, $\beta 1_g(^3P_2) \rightarrow C1_u$, is ≈ 0,[13] hence no interference results.

It is also possible that the lower state is subject to Ω-uncoupling. In the present case, the $A1_u$ state would have to mix with a valence 0_u^+ state in order for the minor component to have a large transition dipole to the dominant component of the upper $E0_g^+(^3P_2)$ state. However, the lowest valence 0_u^+ (the B state) lies $\sim$4000 cm^{-1} above the $A1_u$ state and the mixing is negligible.

IV. CONCLUSIONS

Using high-resolution FT spectroscopy, we have been able to resolve rotational structure in the $D0_u^+(^3P_2) \rightarrow X0_g^+$ emission following collisional transfer from the $E0_g^+(^3P_2)$ state of I_2. The ratio of the intensities of the emission from the two rotational levels populated by $\Delta J = \pm 1$ collisional transfer varies enormously as the vibrational numbering in the $E0_g^+(^3P_2)$ and $D0_u^+(^3P_2)$ states changes. By comparing "wet" and "dry" spectra, we have concluded that the observed intensities are consistent with the transfer being dominated by long-range, resonant collisions with residual H_2O which proves to be unexpectedly difficult to remove from I_2. Unequal *R:P* branch ratios in the direct $E0_g^+(^3P_2) \rightarrow A1_u$ emission have been shown to result from mixing of the $E0_g^+(^3P_2)$ and $\beta 1_g(^3P_2)$ states via Ω-uncoupling.

ACKNOWLEDGMENTS

We would like to thank for Dr. V. Alekseev for drawing our attention to the existence of the earlier (unpublished) FT work, for calculating the vibrational distributions, and for numerous stimulating discussions.

[1] T. Ridley, K. P. Lawley, and R. J. Donovan, J. Chem. Phys. **131**, 234302 (2009).
[2] D. Inard, D. Cerny, M. Nota, R. Bacis, S. Churassy, and V. Skorokhodov, Chem. Phys. **243**, 305 (1999).
[3] V. A. Alekseev, Opt. Spectrosc. **110**, 335 (2011).
[4] J. P. Perrot, B. Femelat, M. Broyer, and J. Chevaleyre, Mol. Phys. **61**, 97 (1987).
[5] F. Martin, R. Bacis, S. Churassy, and J. Vergès, J. Mol. Spectrosc. **116**, 71 (1986).
[6] K. S. Viswanathan, A. Sur, and J. Tellinghuisen, J. Mol. Spectrosc. **86**, 393 (1981).
[7] P. Luc, J. Mol. Spectrosc. **80**, 41 (1980).
[8] J. P. Perrot, M. Broyer, J. Chevaleyre, and B. Femelat, J. Mol. Spectrosc. **98**, 161 (1983).
[9] J. Tellinghuisen, J. Mol. Spectrosc. **217**, 212 (2003).
[10] J. C. D. Brand, A. R. Hoy, A. K. Kalkar, and A. B. Yamashita, J. Mol. Spectrosc. **95**, 350 (1982).
[11] H. M. Randall, D. M. Dennison, N. Ginsburg, and L. R. Weber, Phys. Rev. **52**, 160 (1937).
[12] R. A. Gottscho, J. B. Koffend, R. W. Field, and J. R. Lombardi, J. Chem. Phys. **68**, 4110 (1978).
[13] K. P. Lawley, P. J. Jewsbury, T. Ridley, P. R. R. Langridge-Smith, and R. J. Donovan, Mol. Phys. **75**, 811 (1992).